HHS Public Access

Author manuscript

Immunohorizons. Author manuscript; available in PMC 2023 May 19.

Published in final edited form as:

Immunohorizons. ; 5(12): 918–930. doi:10.4049/immunohorizons.2000087.

Inhibition of H3K27me3 demethylases promotes plasmablast formation

Anna K. Kania[†], **Muyao Guo**[†,‡], **Christopher D. Scharer**[†], **Jeremy M. Boss**[†,*]

[†]Department of Microbiology and Immunology, Emory University School of Medicine, Atlanta, GA 30322, USA

[‡]Currently at Department of Rheumatology and Immunology, Xiangya School of Medicine, Central South University, Changsha, 410008, China

Abstract

B cell differentiation into antibody-secreting plasma cells requires transcriptional, metabolic, and epigenetic remodeling. H3K27me3, a histone modification associated with gene silencing, is dynamically regulated during B cell differentiation. Although several studies have focused on mechanisms involving the gain of this modification in plasmablasts (PB), the role of active demethylation of H3K27me3 by UTX and JMDJ3 during B cell differentiation has not been examined. Here, this process was assessed using a pharmacological inhibitor of UTX and JMJD3, GSK-J4. Treatment of *ex vivo* stimulated mouse B cells with GSK-J4 led to an increase in plasmablast frequency without affecting the ability of the newly formed plasmablasts to secrete antibodies. Consistent with the role of UTX and JMJD3 in promoting gene expression, the majority of differentially expressed were downregulated upon GSK-J4 treatment. GSK-J4-treated cells downregulated genes associated with signaling and P53 pathways. Inhibitor treated cells upregulated genes associated with cell cycle and proliferation, which correlated with an increase in actively proliferating cells. Unexpectedly, a majority of the downregulated transcripts corresponded to genes that in the wild-type setting were genes that gain H3K27me3 and downregulated in PB. Together, our results show that UTX and JMDJ3 are required to restrain B cell differentiation and suggests that they function as a rheostat for H3K27me3 to control this process.

INTRODUCTION

Humoral immunity relies on the ability of naïve B cell (**nB**) to differentiate into antibody secreting short-lived plasmablasts (**PB**) or long-lived post-mitotic plasma cells (**PC**). To allow for robust antibody secretion and differentiation, B cells undergo substantial changes in their transcriptional prolife as well as metabolism (1–4). nB and PC fates are regulated by distinct sets of transcription factors. Whereas PAX5 (5–8) and BACH2 (9, 10) promote the nB stage, BLIMP1 (11–13) and high levels of IRF4 (14, 15) promote PC formation. In addition, there is a growing appreciation for the epigenetic reprograming that occurs during B cell differentiation (16, 17). This is well exemplified by the fact that differentiating B

[*]Correspondence: jmboss@emory.edu; 404-727-5973.

cells undergo cell-division coupled reprogramming of their accessible chromatin landscape and progressive DNA hypomethylation of their genome following stimulation with T-cell independent antigens (18, 19).

In addition to changes in DNA methylation to facilitate cell fate decisions, the distribution of histone modification also changes during B cell differentiation (18, 20, 21). Of particular note is the status of histone H3 lysine 27 trimethylation (H3K27me3) modifications at nB- and PB-specific genes. This histone modification is associated with a repressed chromatin state and gene silencing (22). H3K27me3 is deposited by EZH2 (23–25), a component of the PRC2 complex, and is enzymatically removed by two demethylases UTX (Ubiquitously transcribed tetratricopeptide repeat, X chromosome) and JMJD3 (Jumonji Domain-Containing Protein 3) (26, 27). UTX and JMJD3 are also termed KDM6A and KDM6B, respectively. In a recent study, H3K27me3 was shown to be dynamically regulated during B cell differentiation with roughly equal number of promoter regions that gain and lose this histone modification as B cells differentiate to PB (21). Deposition of H3K27me3 by EZH2 has been shown to play an important role during B cell development (28, 29), germinal center formation and maintenance (30–32), as well as PB formation in response to T-independent antigens (21). However, a significant gap in knowledge persists concerning the role of UTX and JMJD3 in the epigenetic regulation of B cell differentiation and PC formation.

UTX and JMJD3 facilitate H3K27me3 demethylation via their Jumonji C domain in an iron and alpha-ketoglutarate dependent manner (33, 34). This process occurs via direct hydroxylation of the methyl group resulting in a formation of a hydroxymethyl intermediate, which is then released as a formaldehyde (35). UTX is X linked with a homolog, UTY, encoded on the Y chromosome. The demethylation activity of UTY is extremely low compared to UTX (26, 27, 36). In addition to their catalytic activity, UTX and JMJD3 influence gene expression through interactions with a host of chromatin regulators, including BRG1 (37, 38) and CHD4 (38, 39), p300 (40), and most notably the MLL complex, which promotes H3K4 methylation (41, 42). The tumor suppressor p53 also interacts with UTX and JMJD3 (43). UTX and JMJD3 have been shown to function in various biological processes, including early embryonic development (44–46). Such roles were shown to be in part by facilitating resolution of bivalent promoters at retinoic acid inducible genes (47) and derepressing inactive enhancers (40). Other roles have included cardiac development (48), hematopoiesis (49), M2 macrophages differentiation (50), and regulation of various T cell subsets (37, 51–56).

In a clinical setting, mutations in *UTX* lead to a rare, congenital disorder characterized by distinct facial features, developmental delay, intellectual disability, and multi-organ malfunctions (57, 58). Furthermore, mutations in *UTX* have been identified in Diffuse Large B-cell Lymphoma (DLBCL) (59) and multiple myeloma (60–62). Mutations in JMJD3 have been described in Hodgkin's Lymphomas (63) and DLBCL (64, 65). Together, this suggests that these enzymes are important regulators of B cell fate. Furthermore, changes in the expression of genes associated with PC and memory B cells have been reported following overexpression of JMJD3 in human germinal center B cells (63). However, the role of UTX

and JMJD3 in B cell differentiation has not been fully examined, thus leaving a significant gap in our knowledge of epigenetic regulation of PC formation.

In this study, we utilized a pharmacological inhibitor for UTX and JMJD3 to examine their role in regulating B cell differentiation using an *ex vivo* model system. The results showed that the demethylation enzymes are involved in controlling cell cycle, proliferation, and ultimately the frequency of B cells that differentiate into PB and are therefore critical for PB reprogramming and function.

METHODS

Mice

C57BL/6J mice (Stock# 000664) were purchased from Jackson Labs and bred on site. All animals were housed by the Emory Division of Animal Resources following protocols approved by the Emory Institutional Animal Care and Use Committee.

Ex vivo differentiation

Naïve splenic B cells were magnetically enriched by negative selection using CD43 (Ly-48) MicroBeads (Miltenyi Biotec 130-097-148) with >95% purity. Unless otherwise stated, purified B cells were cultured at 0.5×10^6 cells/ml of B cell media (RPMI 1640, 10% heat-inactivated FBS, 0.05 mM 2-ME, 1X nonessential amino acids, 1X penicillin/streptomycin, 10 mM HEPES, and 1 mM sodium pyruvate) supplemented with 20 μg/ml LPS (Sigma L2630), 20 ng/ml IL-2 (Biolegend 575406), and 5 ng/ml IL-5 (Biolegend 581504). LPS and cytokines were supplemented with half the above dose at 24 and 48hr of *ex vivo* culture as previously described (66). In some experiments, naïve B cells were stained with 5μM Cell Trace Violet (Life Technologies C34557) prior to culturing. GSK-J4 (Sigma SML0701) and GSK-J5 (Cayman Chemical, 12074) were dissolved in DMSO and diluted in B cell media. Cells were treated daily with 250nM GSK-J4 or DMSO. For CD40L stimulation, cells were seeded at 10^5 cells/ml in the above B-cell media containing CD40L (100 ng/ml, R&D Systems), IL-5 (5 ng/ml) and IL-4 (20 ng/ml, R&D Systems). Cultures were supplemented with the cytokines at each subsequent day of culture. For bromodeoxyuridine (BrdU) cell cycle analysis, cells were washed, resuspended in fresh media containing 10 μM BrdU, and incubated at 37°C for two hours. Cell proliferation analysis then performed using Phase-Flow FITC BrdU Kit following the manufacturer's protocol (Biolegend 370704).

Flow Cytometry

Cells were resuspended at 10^6 per 100μl of FACS buffer (1X PBS, 1%BSA, and 2mM EDTA) and blocked with anti-Fc (anti-CD16/CD32) (Tonbo Biosciences, 2.4G2). The following antibodies were used to for staining: B220-PE-Cy7 (Tonbo Biosciences RA3-6B2), CD138-BV711 (BD, 281–2), GL7 eFluor660 (eBioscience, GL-7), CD11b-FITC (Tonbo Biosciences, M1/70), and Ghost Dye™ Red 780 (Tonbo Biosciences 13–0865) to asses viability. The Annexin V FITC Apoptosis Detection Kit (eBioscience BMS500FI-100) was used to assess cell death. Cells were stained for 40 min and fixed using 1% paraformaldehyde.

Enrichment of CD138+ PB was performed by staining with CD138-APC (BD, 281–2), followed by magnetic enrichment using anti-APC MicroBeads (Miltenyi # 130-090-855). For RNA-seq, GL7+ cells were further enriched from the CD138-depleted fractions using GL7-PE (Biolegend #144608) and anti-PE MicroBeads (Miltenyi #130-105-639).

Flow cytometry was performed on a BD LSRII using FACSDiva (v6.2) and analyzed using FlowJo software. The following gating strategy preceded all flow cytometry analyses presented. Cells were gated on 1) lymphocytes (forward light scatter [FSC]–area by side scatter [SSC]–area), 2) singlets (FSC-height by FSC- width), 3) singlets (SSC- height by SSC-width), 4) live cells (Viability Dye negative), with 5) the exclusion of contaminating macrophages bearing CD11b (Supplemental Figure2A).

Western Blot

Ex vivo cultured B cells were lysed on ice in RIPA buffer (150mM NaCl, 0.5% sodium deoxycholate, 0.1% SDS, 1% IGEPAL, 20% glycerol, 50mM Tris pH 8.0) for 20 min. Protein concentration was determined by a Bradford assay (BioRad Inc.). Primary antibody incubation was conducted at 4° C overnight, followed by several washes and a one-hour incubation with the secondary antibody. The following antibodies were used: anti-UTX (Cell Signaling, 33510S), anti-JMJD3 (LSBio, C96528), anti-KDM5B (Abcam, ab181089), anti-KDM5C (Proteintech 14426-1-AP), and anti-ACTIN (Santa Cruz, sc69877). Blots were developed using the Immunobilon Cresendo HRP Substrate (Sigma, WBLURO100) and visualized on Biorad ChemiDoc MP Imaging System.

Enzyme-Linked Immunosorbent Assay (ELISA)

Equal numbers of DMSO- or GSK-J4-treated plasmablasts were cultured in fresh B cell media. After 2.5hr, the supernatant was collected and used to perform ELISA. ELISA plates (Sigma M9410) were coated with goat anti-mouse Ig (Southern Biotechnology 5300-05B) overnight at 4° C and blocked with 3% nonfat dry milk. Standard IgM antibody (Southern Biotechnology 5300-01B) and collected media supernatants were incubated for 2 hr at room temperature, followed by washes, and incubation with HRP-conjugated goat anti-mouse secondary antibody (Southern Biotechnology 1021-05) for 2 hr at room temperature. The plates were developed using the TMB ELISA peroxidase substrate (Rockland 800-666-7625) and the reaction was stopped using 0.2M sulfuric acid. Plates were read using a Synergy HT Multi-Mode Microplate Reader (BioTek).

RNA-seq

RNA was isolated from magnetically enriched PB and ActB using Zymo Quick-RNA MicroPrep Kit (11-328M). Sequencing libraries were generated using mRNA HyperPrep Kit (KAPA Biosystems KR1352) with 500ng input RNA per sample. Final libraries were quality checked on a bioanalyzer, quantitated by quantitative PCR (qPCR), pooled at equimolar ratio, and sequenced on a HiSeq2500 using paired- end, 50-bp sequencing chemistry. TopHat2[27] was used to map the raw sequencing reads to the mm9 mouse genome. For each sample, reads that overlapped exons of unique ENTREZ genes were annotated using the GenomicRanges (v1.22.4) package in R/Bioconductor. Differential expression analysis was performed using Bioconductor package edgeR using FDR ≤ 0.05 and 1.5-fold change

($log_2 = 0.58$) (Supplemental Table 1). PCA was performed using vegan package and the indicated z-score normalized gene list. For gene set enrichment analysis (GSEA)(67), all detected genes were ranked by multiplying the sign of fold change by the −log10 (P value).

Data and Code Availability

All sequencing data have been deposited in NCBI Gene Expression Omnibus (GEO) under the accession codes GSE158139. Code and data processing scripts are available from the corresponding author upon request and at https://github.com/cdschar/.

RESULTS

H3K27me3 demethylases are upregulated during B cell differentiation

Previous work (21) described significant gains and losses in H3K27me3 modifications as B cells differentiated to PB in response to LPS, pointing to a potential role for the removal of these marks by histone demethylases. The expression of the two H3K27me3 demethylases (UTX and JMJD3) was examined in a previously published data set (68), which quantified gene expression during *in vivo* differentiation of nB following LPS stimulation. Analysis of this data revealed that compared to nB, *Utx* was upregulated several fold in newly formed plasmablasts (PB), while *Jmjd3* expression showed a modest albeit statistically significant increase in expression (Figure 1A). Expression of UTX and JMJD3 was also examined in a second LPS-induced *in vivo* B-cell differentiation model dataset that correlated gene expression as a function of cell division (19). In that system, PB form after division 8 and are phenotypically recognized by expression of the plasma cell maker CD138 (termed division 8+). Again, *Utx* expression was significantly higher in the division 8+ cells, which represent the newly formed PB compared to control earlier divisions (Figure 1B). Furthermore, consistent with the changes in gene expression, the protein levels of UTX and JMJD3 were higher in PB derived from *ex vivo* cultures compared to nB and not altered in expression by GSK-J4 treatment (Supplemental Figure 1A). In a similar manner, other histone modifiers that are known to be functionally affected by GSK-J4 were not altered in expression by the inhibitor (Supplemental Figure 1A). To determine whether change in H3K27me3 during B cell differentiation correlated with transcriptional differences, the change in promoter H3K27me3 enrichment (21) was plotted against the change in gene expression between nB and PB (68). Consistent with the repressive role of H3K27me3, the analysis revealed two major sets of genes: 1) genes that had high expression and low H3K27me3 levels in PB (Figure 1C; green quadrant); and 2) genes that had low expression and high H3K27me3 in PB compared to nB (Figure 1C; blue quadrant). H3K27me3 enrichment at the abovementioned gene groups was quantified (Figure 1D). This analysis also revealed a group of genes that were upregulated in PB but exhibited a higher level of promoter H3K27me3 (Figure 1C; gray shade) and are therefore not likely to be regulated by this histone modification but rather by other epigenetic or transcriptional mechanisms.

To study the role of UTX and JMDJ3 during B cell differentiation, a pharmacological inhibitor, GSK-J4, known to inhibit the activity of these enzymes was utilized (69). In this system, naïve B cells were differentiated *ex vivo* with LPS, IL-2, and IL-5 as previously described (66).

Treatment with GSK-J4 promotes PB formation

To examine the effect of the inhibitor-mediated loss of UTX and JMJD3 catalytic activity on B cell differentiation, nB were isolated and stimulated *ex vivo* with LPS, IL-2, and IL-5 in the presence of 250nM GSK-J4 or DMSO control. After three days of culture, flow cytometry analysis revealed a significant increase in the frequency of CD138+ PB in the GSK-J4 treated cultures (Figure 2A) with a small but significant increase in the B220+GL7+ activated B cells (**ActB**) (Figure 2B). Importantly, an increase in PB following GSK-J4 treatment was also observed when compared to the inactive control compound, GSK-J5 (Figure 2C). To determine whether the observed phenotype was specific to TLR signaling, the effect of inhibitor treatment on PB formation was examined following stimulation with CD40L, IL-4, and IL-5 that mimic T-cell dependent B cell activation (70). Enhanced B cell differentiation was also observed following this mode of stimulation (Figure 2D).

To determine whether the UTX/JMJD3 inhibition affected the ability of cells to secrete antibodies, CD138+ PB from the LPS cultures were magnetically enriched after three days of *ex vivo* culture and an equal number of cells was plated in fresh media. Antibody secretion was then analyzed by ELISA and revealed no difference in the IgM antibody titers between the GSK-J4 and DMSO treated PB (Figure 2E), suggesting that UTX/JMJD3 regulate the process of B cell differentiation but not the antibody secreting function of PB.

Inhibitor treatment alters B cell transcriptome

To define the mechanism by which treatment with GSK-J4 promotes B cell differentiation, RNA-seq was performed on magnetically enriched nB, as well ActB and PB derived from GSK-J4 or DMSO cultures at day 3 post LPS, IL-2, and IL-5 stimulation (Supplemental Figure 2B). Principal component analysis (**PCA**) revealed that the activation status was the major source of variation as principal component (PC) 1 separated nB from ActB and PB. PC2 separated ActB from PB, while PC3 stratified cells based on GSK-J4 treatment status (Figure 3A). Consistent with results of PCA, hierarchical clustering of samples and differentially expressed genes (DEG) between GSK-J4 and DMSO revealed that samples stratified based on cells type rather than treatment status (Figure 3B). Differential expression analysis of GSK-J4 and DMSO treated cells (1.5-fold change, FDR <0.05) revealed a skewing towards genes downregulated following drug treatment. In the ActB comparison, 253 genes were downregulated (**downDEG**) and 106 were upregulated (**upDEG**). In the PB comparison, there were 352 downDEG and 84 upDEG (Figure 3C; Supplemental Table 1). Furthermore, a common set of 113 genes was downregulated in both comparisons (Figure 3D). The observed enrichment for downregulated genes is consistent with inhibition of UTX and JMJD3, which in the wild-type setting promote gene expression. GSK-J4 has been shown to act, although with weaker activity, on KDM5B and KDM5C, the H3K4me2/3 demethylases (69, 71). However, inhibition of H3K4me3 demethylases would be predicted to result in gene upregulation. Thus, this observation suggests that the inhibitor primarily acts on the UTX and JMJD3 demethylase pathway rather than others.

To identify the pathways altered following GSK-J4 treatment, gene set enrichment analysis (**GSEA**) (67) was performed on a ranked gene list for the ActB GSK-J4 v ActB DMSO comparison. This analysis revealed downregulation of genes associated with hypoxia, TNF

signaling, P53 pathways, and apoptosis (Figure 3E). Examples of genes downregulated following inhibitor treatment included *Cdkn2a*, encoding $p16^{Ink4a}$ and $p19^{Arf}$, which inhibit the G1/S cell cycle transition (72) and regulate p53 stability (73), respectively. Other examples of down regulated DEG include *Bnip3l*, which promotes apoptosis (74), and *Pdk1*, which inactivates pyruvate dehydrogenase, thereby inhibiting the conversion of pyruvate into acetyl-CoA (75, 76) (Figure 3F). Despite dysregulation of several apoptotic factors, there was no difference in the frequency of apoptotic cells following inhibitor treatment. A small but significant increase in necrotic cells at 48hr post stimulation was observed (Supplemental Figure 1B and C), but this difference does not explain differences observed in the number of plasmablasts formed (Figure 2A and C).

Additionally, cell cycle and proliferation genes were upregulated following inhibitor treatment (Figure 3G). Some of the pathways dysregulated have been previously shown to be downregulated in the absence of EZH2 (21) and are upregulated as B cells progress through cell division and differentiate to PB (19). This suggested that the PB program may be initiated early or more strongly in GSK-J4 treated cells. To test this, expression of genes that were previously described to constitute a PC transcriptional signature was examined in inhibitor treated cells (77). GSEA analysis revealed upregulation of PC-signature genes in inhibitor treated ActB and PB (Figure 3H, Figure 3I, Supplemental Figure 1D). Taken together, GSK-J4 led to global changes in the B cell transcriptome, indicating a role for H3K27 demethylation in regulating the PB transcriptome.

Inhibitor treated cells exhibit increased proliferation

The downregulation of *Cdkn2a* and the p53 pathway combined with an upregulation of genes associated with cell cycle and proliferation following GSK-J4 treatment, led to the hypothesis that inhibitor treatment results in enhanced proliferation. To examine whether treatment with GSK-J4 altered cell division kinetics, nB were stained with CellTrace Violet (CTV) and stimulated *ex vivo* with LPS, IL-2, IL-5 in the presence of GSK-J4 or DMSO. Irrespective of treatment, cultured B cells underwent six cell divisions after three days of culture. However, analysis of PB frequency at each division revealed a significant increase in PB per division following inhibitor treatment, with PB increasing as early as division four (Figure 4A). To examine whether inhibitor treatment altered cell cycle distribution in treated cells, at day 3 post LPS stimulation, B cell cultures were pulsed with bromodeoxyuridine (**BrdU**) for 2 hours and analyzed by flow cytometry. GSK-J4 treatment led to a significant increase in the frequency of cells in the S phase of the cell cycle (Figure 4B). Further, analysis of BrdU by cell division revealed a significant increase in the frequency of BrdU+ cells at the early cell divisions (Figure 4C). Overall, while GSK-J4 treatment does not alter the total number of cell divisions, it does lead to an increase in actively proliferating cell (S phase cell cycle) with a proportional reduction of cells in the G1 phase.

DEG are enriched for genes regulated by H3K27me3

To determine whether inhibition of UTX and JMJD3 predominately affects genes regulated by H3K27me3 during B cell differentiation, genes downregulated in PB following GSK-J4 treatment were overlaid on the scatterplot comparing PB/nB gene expression vs change in H3K27me3 enrichment in Figure 1. Consistent with the hypothesis that UTX and JMJD3

promote demethylation of H3K27me3 at genes upregulated in PB, several of GSK-J4 downDEG fell in the “green” quadrant described above. This group includes genes such as *Slc7a3*, which encodes a sodium-independent transporter of cationic amino acids (78, 79) (Figure 5A, 5C). Other genes included *Cth* (80), *Lars2* (81), *Ddt* (82), *Fut1, Tmed6* (83), *Galk1*(84), *Gstt1* (85), *Abcb8* (86), that are involved in various aspects of protein synthesis or protein modification, secretion, vesicular trafficking and metabolism. Unexpectedly, the majority of the genes downregulated following inhibitor treatment correspond to genes that in the wild-type setting gain promoter H3K27me3 and are downregulated in PB (“blue” quadrant) (Figure 5A). H3K27me3 levels at GSK-J4 downDEG in the respective quadrants was quantified (Figure 5B). Thus, genes downregulated by inhibition of UTX and JMJD3 are predominately enriched for regions that in the wild-type setting gain H3K27me3 during B cells differentiation. Due to the gain in H3K27me3, these genes are likely regulated in part by EZH2, which is the counterpart to UTX/JMJD3. In fact, GSK-J4 downDEG genes in the “blue” quadrant corresponded to genes that were significantly upregulated in EZH2-deficient PB and 29% were defined as DEG (21) (Figure 5C).

Examples of genes that are downregulated following GSK-J4 and have high levels of H3K27me3 in wild-type PB include *Id3* (inhibitor of DNA-binding/differentiation 3), which forms heterodimers with E box proteins to inhibit their DNA binding (87), is normally repressed during plasma cell formation with concomitant accumulation of H3K27me3. Following GSK-J4 treatment, *Id3* expression is super repressed in the PB (Figure 5D top). *Spib*, which regulates the ability of B cells to respond to external stimulation and inhibits germinal center B cell and PB formation (88), followed a similar path, normally accumulating H3K27me3 in PB and was super repressed in GSK-J4 treated PB (Figure 5D bottom). Together, these data suggest that inhibition of UTX and JMJD3 leads to enhanced repression of a subset of B cell fate genes that gain H3K27me3, thus promoting PB formation.

To evaluate whether genes upregulated following inhibitor treatment were enriched for genes regulated by H3K4me3, we overlaid genes upregulated in PB following inhibitor treatment on a scatterplot comparing PB/nB gene expression (68) versus change in H3K4me3 enrichment (18) in a manner similar to Figure 5A. A majority of the GSK-J4 upDEG corresponded to genes that exhibited minimal, if any, change in H3K4me3 methylation during B cell differentiation (Figures 5F and 5G). Thus, the data strongly suggest the genes upregulated following inhibitor treatment are the result of inhibiting H3K4me3 demethylases.

DISCUSSION

This study investigated the role of histone H3K27me3 demethylation by UTX and JMJD3 on B cell differentiation through the use of GSK-J4, a pharmacological inhibitor that functions as a competitor for their substrate α-ketoglutarate (69). GSK-J4 was previously shown to display high specificity for UTX and JMJD3 and H3K27me3 demethylation and acted at a lower specificity towards H3K4me3 demethylases (69, 71). GSK-J4 treatment of nB cells stimulated with LPS, IL-2, and IL-5 led an increase in the frequency of PB and dysregulation in gene expression. Despite promoting PB formation, GSK-J4 treatment had

no influence on the ability of treated cells to secrete antibodies. At the molecular level, GSK-J4 treatment during the differentiation process led to more genes being down regulated than expected. This observation suggests that the changes are likely driven by inhibition of UTX and JMJD3, which by removal of the inhibitory histone mark H3K27me3 normally promote gene expression. Some of these dysregulated genes included those associated with hypoxia, signaling, apoptosis, and P53 pathways, including cell cycle inhibitor *Cdkn2a* (72). The transcription factors SPIB and ID3, which are known PB repressors (70, 88), were also downregulated and may account for the upregulation of PC-signature genes. Other genes found to be upregulated by GSK-J4 treatment during the differentiation process were associated with cell cycle and proliferation. These changes in gene expression were correlated with an increase of actively proliferating BrdU+ cells following GSK-J4 treatment of *ex vivo* differentiated nB. Thus, targeting cell cycle inhibitors and PB repressors are in part responsible for the increases in PB appearing following inhibition of these demethylases.

Epigenetic remodeling is necessary during B cell differentiation (18, 20, 21), and the histone modification H3K27me3 shows dynamic changes at thousands of loci with sites both gaining and losing the mark. A majority of GSK-J4 down modulated DEG were associated with changes in promoter localized H3K27me3 – although other changes can be observed in the gene body – during the differentiation process. This observation is consistent with the active and direct demethylase activities of UTX and JMDJ3 in which a subset of GSK-J4 downDEG corresponded to genes that normally lose promoter H3K27me3 and gain expression as B cells differentiate. Surprisingly, a number of GSK-J4 down modulated DEG matched genes that normally gain promoter H3K27me3 and are downregulated as B cells differentiate to PB. This included transcription factors known to repress the PB fate. Thus, UTX and JMJD3 might function as the rheostat or counterbalance for H3K27me3 by counteracting the activity of EZH2, the H3K27 methyltransferase. Taken together, these data suggest that the level of promoter H3K27me3 and gene expression during B cell differentiation is modulated by three distinct mechanisms: 1) direct control of a gene by either UTX/JMJD3 or EZH2; 2) a balanced control in gene expression in which both UTX/JMJD3 and EZH2 compete for the same genes, resulting in fine tuning of gene expression; or 3) indirect control of gene expression through passive loss of H3K27me3 through cell division in which EZH2 is no longer recruited to a locus.

There is growing evidence that the balance in the levels of histone modifications are necessary for proper B cell differentiation. Methylation of H3K4 is associated with gene activation and has been shown to play a critical role in B cells (89). Deletion of *Kmt2d*, the H3K4 methyltransferase, led to an increase in germinal center B cells as a result of enhanced proliferation capacity of follicular B cells lacking *Kmt2d* (90). Deletion of LSD1, the H3K4me1/2 demethylase, resulted in the opposite phenotype. B cells lacking LSD1 showed reduced proliferation and differentiation following T cell independent stimulation (68), as well as reduced germinal center B cells (91). In a similar scenario, deletion of EZH2 resulted in reduction in germinal center and plasma cell formation and reduced proliferation (21, 30, 31); whereas, here, inhibition of UTX and JMJD3 led to increased PB formation and enhanced cell proliferation. Together, these results suggest that balanced level

of opposing histone modifications is necessary for maintaining B cell fate and controlling cell proliferation.

The importance of balanced levels of histone modification is well exemplified by the fact that mutations in various epigenetic modifiers are frequently found in cancer (92). In particular, gain of function mutations in *EZH2* have been identified in various human malignancies, including DLBCL, which results in increased promoter H3K27me3 methylation at cell cycle checkpoint genes including *CDKN1A* and genes associated with germinal center exit (30). However, mutations in *UTX* are typically loss-of-function or deletion, which leads to a failure to demethylate H3K27me3. This results in increased levels of H3K27me3, possibly mimicking EZH2 hyperactivation (61, 93). Furthermore, attempts to re-establish a homeostatic level of this histone modification have proved to be an effective therapeutic avenue for human cancers as EZH2 inhibitors are in clinical use and ongoing trials (94). A recent study has also proposed the use of EZH2 inhibitors for malignancies with UTX loss-of-function mutations. Treatment with EZH2 inhibitors led to reduced viability and cell cycle arrest of multiple myeloma cell lines lacking *UTX* and resulted in reduced tumor burden *in vivo* (62). Taken together, the balanced level of H3K27me3 is necessary to maintain homeostatic and prevent development human malignancies.

The role of UTX and JMJD3 has been examined in various cells types, including the hemopoietic lineage. Interestingly, several studies revealed demethylase independent roles for these enzymes in addition to their known role in active demethylation. The demethylase activity of UTX is required for the formation of invariant natural killer T cells; however, in mouse embryonic stem cells UTX cooperates with MLL4 complex and p300 to convert enhancers from an inactive to active state. This action occurs in the absence of the demethylase activity of UTX. In this setting, UTX promotes and enhances the activity of its binding partners to promote H3K4me1 and H3K27ac at enhancers (40). The inhibitor utilized in this study targets the catalytic activity of UTX and JMJD3 thus allowing for a targeted analysis of active H3K27me3 demethylation by both enzymes during B cell differentiation.

While the presented data strongly suggest that the observed increase in PB is the result of the inhibition H3K27me3 demethylases, the GSK-J4 has also been shown to act on other histone demethylase (69, 71). As such, it is remains possible that the observed PB following GSK-J4 is a cumulative effect of inhibiting multiple demethylases, including UTX and JMDJ3. The development of new compounds specifically targeting the H3K27me3 demethylases is necessary to more definitely address the role of inhibition of UTX and JMJD3 in B cell differentiation.

Mutations in *UTX* and *JMJD3* have been reported in various cancers and several studies identified GSK-J4 as a potential therapeutic treatment for a subset of malignancies driven by gain of function mutations in these genes (64, 95, 96). Despite the promising effects of GSK-J4 as a cancer treatment, this drug is not currently used in any clinical trials, likely due to its non-specific activity towards other demethyalses. The work presented here would suggest that targeted UTX/JMJD3 inhibition could result in increased PB and PC formation that may exacerbate normal immune responses in treated patients.

In summary, the work described here demonstrates an important balance in the control of gene expression potentially regulated by the placement and removal of repressive histone modifications at histone H3K27. The dynamic changes in this histone modification at the targeted loci are likely critical for maintaining the cell fates as a B cell or as plasma cells following their complex differentiation process.

Supplementary Material

Refer to Web version on PubMed Central for supplementary material.

Acknowledgements

We thank members of the Boss lab for critical reading of the manuscript and Royce Butler for animal husbandry.

This work was supported by National Institute of Health grants: RO1 AI123733 and P01 AI125180 to J.M.B, T32 GM0008490 to A.K.K.

Abbreviations

nB	naïve B cells
ActB	activated B cell
PB	plasmablast
PC	plasma cell
CTV	Cell Trace Violet
BrdU	bromodeoxyuridine
RNA-seq	RNA sequencing
DEG	differentially expressed gene
upDEG	upregulated differentially expressed gene
downDEG	downregulated differentially expressed gene
FDR	false discovery rate
GSEA	gene set enrichment analysis
ELISA	Enzyme-Linked Immunosorbent Assay
FSC	forward light scatter
SSC	side scatter

REFERENCES

1. Nutt SL, Hodgkin PD, Tarlinton DM, and Corcoran LM. 2015. The generation of antibody-secreting plasma cells. Nat Rev Immunol 15: 160–171. [PubMed: 25698678]

2. Fairfax KA, Kallies A, Nutt SL, and Tarlinton DM. 2008. Plasma cell development: from B-cell subsets to long-term survival niches. Semin Immunol 20: 49–58. [PubMed: 18222702]

3. Boothby M, and Rickert RC. 2017. Metabolic Regulation of the Immune Humoral Response. Immunity 46: 743–755. [PubMed: 28514675]

4. Lam WY, and Bhattacharya D. 2018. Metabolic Links between Plasma Cell Survival, Secretion, and Stress. Trends Immunol 39: 19–27. [PubMed: 28919256]

5. Nutt SL, Heavey B, Rolink AG, and Busslinger M. 1999. Commitment to the B-lymphoid lineage depends on the transcription factor Pax5. Nature 401: 556–562. [PubMed: 10524622]

6. Usui T, Wakatsuki Y, Matsunaga Y, Kaneko S, Koseki H, and Kita T. 1997. Overexpression of B cell-specific activator protein (BSAP/Pax-5) in a late B cell is sufficient to suppress differentiation to an Ig high producer cell with plasma cell phenotype. J Immunol 158: 3197–3204. [PubMed: 9120274]

7. Lin KI, Angelin-Duclos C, Kuo TC, and Calame K. 2002. Blimp-1-dependent repression of Pax-5 is required for differentiation of B cells to immunoglobulin M-secreting plasma cells. Mol Cell Biol 22: 4771–4780. [PubMed: 12052884]

8. Nera KP, Kohonen P, Narvi E, Peippo A, Mustonen L, Terho P, Koskela K, Buerstedde JM, and Lassila O. 2006. Loss of Pax5 promotes plasma cell differentiation. Immunity 24: 283–293. [PubMed: 16546097]

9. Muto A, Tashiro S, Nakajima O, Hoshino H, Takahashi S, Sakoda E, Ikebe D, Yamamoto M, and Igarashi K. 2004. The transcriptional programme of antibody class switching involves the repressor Bach2. Nature 429: 566–571. [PubMed: 15152264]

10. Ochiai K, Muto A, Tanaka H, Takahashi S, and Igarashi K. 2008. Regulation of the plasma cell transcription factor Blimp-1 gene by Bach2 and Bcl6. Int Immunol 20: 453–460. [PubMed: 18256039]

11. Shapiro-Shelef M, Lin KI, McHeyzer-Williams LJ, Liao J, McHeyzer-Williams MG, and Calame K. 2003. Blimp-1 is required for the formation of immunoglobulin secreting plasma cells and pre-plasma memory B cells. Immunity 19: 607–620. [PubMed: 14563324]

12. Kallies A, Hasbold J, Tarlinton DM, Dietrich W, Corcoran LM, Hodgkin PD, and Nutt SL. 2004. Plasma cell ontogeny defined by quantitative changes in blimp-1 expression. J Exp Med 200: 967–977. [PubMed: 15492122]

13. Soro PG, Morales AP, Martinez MJ, Morales AS, Copin SG, Marcos MA, and Gaspar ML. 1999. Differential involvement of the transcription factor Blimp-1 in T cell-independent and -dependent B cell differentiation to plasma cells. J Immunol 163: 611–617. [PubMed: 10395648]

14. Ochiai K, Maienschein-Cline M, Simonetti G, Chen J, Rosenthal R, Brink R, Chong AS, Klein U, Dinner AR, Singh H, and Sciammas R. 2013. Transcriptional regulation of germinal center B and plasma cell fates by dynamical control of IRF4. Immunity 38: 918–929. [PubMed: 23684984]

15. Sciammas R, Shaffer AL, Schatz JH, Zhao H, Staudt LM, and Singh H. 2006. Graded expression of interferon regulatory factor-4 coordinates isotype switching with plasma cell differentiation. Immunity 25: 225–236. [PubMed: 16919487]

16. Li G, Zan H, Xu Z, and Casali P. 2013. Epigenetics of the antibody response. Trends Immunol 34: 460–470. [PubMed: 23643790]

17. Zan H, and Casali P. 2015. Epigenetics of Peripheral B-Cell Differentiation and the Antibody Response. Front Immunol 6: 631. [PubMed: 26697022]

18. Scharer CD, Barwick BG, Guo M, Bally APR, and Boss JM. 2018. Plasma cell differentiation is controlled by multiple cell division-coupled epigenetic programs. Nat Commun 9: 1698. [PubMed: 29703886]

19. Barwick BG, Scharer CD, Bally APR, and Boss JM. 2016. Plasma cell differentiation is coupled to division-dependent DNA hypomethylation and gene regulation. Nat Immunol 17: 1216–1225. [PubMed: 27500631]

20. Minnich M, Tagoh H, Bonelt P, Axelsson E, Fischer M, Cebolla B, Tarakhovsky A, Nutt SL, Jaritz M, and Busslinger M. 2016. Multifunctional role of the transcription factor Blimp-1 in coordinating plasma cell differentiation. Nat Immunol 17: 331–343. [PubMed: 26779602]

21. Guo M, Price MJ, Patterson DG, Barwick BG, Haines RR, Kania AK, Bradley JE, Randall TD, Boss JM, and Scharer CD. 2018. EZH2 Represses the B Cell Transcriptional Program and

Regulates Antibody-Secreting Cell Metabolism and Antibody Production. J Immunol 200: 1039–1052. [PubMed: 29288200]

22. Cao R, Wang L, Wang H, Xia L, Erdjument-Bromage H, Tempst P, Jones RS, and Zhang Y. 2002. Role of histone H3 lysine 27 methylation in Polycomb-group silencing. Science 298: 1039–1043. [PubMed: 12351676]
23. Czermin B, Melfi R, McCabe D, Seitz V, Imhof A, and Pirrotta V. 2002. Drosophila enhancer of Zeste/ESC complexes have a histone H3 methyltransferase activity that marks chromosomal Polycomb sites. Cell 111: 185–196. [PubMed: 12408863]
24. Muller J, Hart CM, Francis NJ, Vargas ML, Sengupta A, Wild B, Miller EL, O'Connor MB, Kingston RE, and Simon JA. 2002. Histone methyltransferase activity of a Drosophila Polycomb group repressor complex. Cell 111: 197–208. [PubMed: 12408864]
25. Kuzmichev A, Nishioka K, Erdjument-Bromage H, Tempst P, and Reinberg D. 2002. Histone methyltransferase activity associated with a human multiprotein complex containing the Enhancer of Zeste protein. Genes Dev 16: 2893–2905. [PubMed: 12435631]
26. Hong S, Cho YW, Yu LR, Yu H, Veenstra TD, and Ge K. 2007. Identification of JmjC domain-containing UTX and JMJD3 as histone H3 lysine 27 demethylases. Proc Natl Acad Sci U S A 104: 18439–18444. [PubMed: 18003914]
27. Lan F, Bayliss PE, Rinn JL, Whetstine JR, Wang JK, Chen S, Iwase S, Alpatov R, Issaeva I, Canaani E, Roberts TM, Chang HY, and Shi Y. 2007. A histone H3 lysine 27 demethylase regulates animal posterior development. Nature 449: 689–694. [PubMed: 17851529]
28. Su IH, Basavaraj A, Krutchinsky AN, Hobert O, Ullrich A, Chait BT, and Tarakhovsky A. 2003. Ezh2 controls B cell development through histone H3 methylation and Igh rearrangement. Nat Immunol 4: 124–131. [PubMed: 12496962]
29. Mandal M, Powers SE, Maienschein-Cline M, Bartom ET, Hamel KM, Kee BL, Dinner AR, and Clark MR. 2011. Epigenetic repression of the Igk locus by STAT5-mediated recruitment of the histone methyltransferase Ezh2. Nat Immunol 12: 1212–1220. [PubMed: 22037603]
30. Beguelin W, Popovic R, Teater M, Jiang Y, Bunting KL, Rosen M, Shen H, Yang SN, Wang L, Ezponda T, Martinez-Garcia E, Zhang H, Zheng Y, Verma SK, McCabe MT, Ott HM, Van Aller GS, Kruger RG, Liu Y, McHugh CF, Scott DW, Chung YR, Kelleher N, Shaknovich R, Creasy CL, Gascoyne RD, Wong KK, Cerchietti L, Levine RL, Abdel-Wahab O, Licht JD, Elemento O, and Melnick AM. 2013. EZH2 is required for germinal center formation and somatic EZH2 mutations promote lymphoid transformation. Cancer Cell 23: 677–692. [PubMed: 23680150]
31. Caganova M, Carrisi C, Varano G, Mainoldi F, Zanardi F, Germain PL, George L, Alberghini F, Ferrarini L, Talukder AK, Ponzoni M, Testa G, Nojima T, Doglioni C, Kitamura D, Toellner KM, Su IH, and Casola S. 2013. Germinal center dysregulation by histone methyltransferase EZH2 promotes lymphomagenesis. J Clin Invest 123: 5009–5022. [PubMed: 24200695]
32. Beguelin W, Teater M, Gearhart MD, Calvo Fernandez MT, Goldstein RL, Cardenas MG, Hatzi K, Rosen M, Shen H, Corcoran CM, Hamline MY, Gascoyne RD, Levine RL, Abdel-Wahab O, Licht JD, Shaknovich R, Elemento O, Bardwell VJ, and Melnick AM. 2016. EZH2 and BCL6 Cooperate to Assemble CBX8-BCOR Complex to Repress Bivalent Promoters, Mediate Germinal Center Formation and Lymphomagenesis. Cancer Cell 30: 197–213. [PubMed: 27505670]
33. Jones SE, Olsen L, and Gajhede M. 2018. Structural Basis of Histone Demethylase KDM6B Histone 3 Lysine 27 Specificity. Biochemistry 57: 585–592. [PubMed: 29220567]
34. Sengoku T, and Yokoyama S. 2011. Structural basis for histone H3 Lys 27 demethylation by UTX/KDM6A. Genes Dev 25: 2266–2277. [PubMed: 22002947]
35. Klose RJ, Kallin EM, and Zhang Y. 2006. JmjC-domain-containing proteins and histone demethylation. Nat Rev Genet 7: 715–727. [PubMed: 16983801]
36. Walport LJ, Hopkinson RJ, Vollmar M, Madden SK, Gileadi C, Oppermann U, Schofield CJ, and Johansson C. 2014. Human UTY(KDM6C) is a male-specific N-methyl lysyl demethylase. J Biol Chem 289: 18302–18313. [PubMed: 24798337]
37. Miller SA, Mohn SE, and Weinmann AS. 2010. Jmjd3 and UTX play a demethylase-independent role in chromatin remodeling to regulate T-box family member-dependent gene expression. Mol Cell 40: 594–605. [PubMed: 21095589]

38. Gozdecka M, Meduri E, Mazan M, Tzelepis K, Dudek M, Knights AJ, Pardo M, Yu L, Choudhary JS, Metzakopian E, Iyer V, Yun H, Park N, Varela I, Bautista R, Collord G, Dovey O, Garyfallos DA, De Braekeleer E, Kondo S, Cooper J, Gottgens B, Bullinger L, Northcott PA, Adams D, Vassiliou GS, and Huntly BJP. 2018. UTX-mediated enhancer and chromatin remodeling suppresses myeloid leukemogenesis through noncatalytic inverse regulation of ETS and GATA programs. Nat Genet 50: 883–894. [PubMed: 29736013]
39. Biswas M, Chatterjee SS, Boila LD, Chakraborty S, Banerjee D, and Sengupta A. 2019. MBD3/NuRD loss participates with KDM6A program to promote DOCK5/8 expression and Rac GTPase activation in human acute myeloid leukemia. FASEB J 33: 5268–5286. [PubMed: 30668141]
40. Wang SP, Tang Z, Chen CW, Shimada M, Koche RP, Wang LH, Nakadai T, Chramiec A, Krivtsov AV, Armstrong SA, and Roeder RG. 2017. A UTX-MLL4-p300 Transcriptional Regulatory Network Coordinately Shapes Active Enhancer Landscapes for Eliciting Transcription. Mol Cell 67: 308–321 e306. [PubMed: 28732206]
41. Cho YW, Hong T, Hong S, Guo H, Yu H, Kim D, Guszczynski T, Dressler GR, Copeland TD, Kalkum M, and Ge K. 2007. PTIP associates with MLL3- and MLL4-containing histone H3 lysine 4 methyltransferase complex. J Biol Chem 282: 20395–20406. [PubMed: 17500065]
42. Issaeva I, Zonis Y, Rozovskaia T, Orlovsky K, Croce CM, Nakamura T, Mazo A, Eisenbach L, and Canaani E. 2007. Knockdown of ALR (MLL2) reveals ALR target genes and leads to alterations in cell adhesion and growth. Mol Cell Biol 27: 1889–1903. [PubMed: 17178841]
43. Akdemir KC, Jain AK, Allton K, Aronow B, Xu X, Cooney AJ, Li W, and Barton MC. 2014. Genome-wide profiling reveals stimulus-specific functions of p53 during differentiation and DNA damage of human embryonic stem cells. Nucleic Acids Res 42: 205–223. [PubMed: 24078252]
44. Welstead GG, Creyghton MP, Bilodeau S, Cheng AW, Markoulaki S, Young RA, and Jaenisch R. 2012. X-linked H3K27me3 demethylase Utx is required for embryonic development in a sex-specific manner. Proc Natl Acad Sci U S A 109: 13004–13009. [PubMed: 22826230]
45. Burgold T, Voituron N, Caganova M, Tripathi PP, Menuet C, Tusi BK, Spreafico F, Bevengut M, Gestreau C, Buontempo S, Simeone A, Kruidenier L, Natoli G, Casola S, Hilaire G, and Testa G. 2012. The H3K27 demethylase JMJD3 is required for maintenance of the embryonic respiratory neuronal network, neonatal breathing, and survival. Cell Rep 2: 1244–1258. [PubMed: 23103168]
46. Shpargel KB, Sengoku T, Yokoyama S, and Magnuson T. 2012. UTX and UTY demonstrate histone demethylase-independent function in mouse embryonic development. PLoS Genet 8: e1002964. [PubMed: 23028370]
47. Dhar SS, Lee SH, Chen K, Zhu G, Oh W, Allton K, Gafni O, Kim YZ, Tomoiga AS, Barton MC, Hanna JH, Wang Z, Li W, and Lee MG. 2016. An essential role for UTX in resolution and activation of bivalent promoters. Nucleic Acids Res 44: 3659–3674. [PubMed: 26762983]
48. Lee S, Lee JW, and Lee SK. 2012. UTX, a histone H3-lysine 27 demethylase, acts as a critical switch to activate the cardiac developmental program. Dev Cell 22: 25–37. [PubMed: 22192413]
49. Thieme S, Gyarfas T, Richter C, Ozhan G, Fu J, Alexopoulou D, Muders MH, Michalk I, Jakob C, Dahl A, Klink B, Bandola J, Bachmann M, Schrock E, Buchholz F, Stewart AF, Weidinger G, Anastassiadis K, and Brenner S. 2013. The histone demethylase UTX regulates stem cell migration and hematopoiesis. Blood 121: 2462–2473. [PubMed: 23365460]
50. Satoh T, Takeuchi O, Vandenbon A, Yasuda K, Tanaka Y, Kumagai Y, Miyake T, Matsushita K, Okazaki T, Saitoh T, Honma K, Matsuyama T, Yui K, Tsujimura T, Standley DM, Nakanishi K, Nakai K, and Akira S. 2010. The Jmjd3-Irf4 axis regulates M2 macrophage polarization and host responses against helminth infection. Nat Immunol 11: 936–944. [PubMed: 20729857]
51. Manna S, Kim JK, Bauge C, Cam M, Zhao Y, Shetty J, Vacchio MS, Castro E, Tran B, Tessarollo L, and Bosselut R. 2015. Histone H3 Lysine 27 demethylases Jmjd3 and Utx are required for T-cell differentiation. Nat Commun 6: 8152. [PubMed: 26328764]
52. Liu Z, Cao W, Xu L, Chen X, Zhan Y, Yang Q, Liu S, Chen P, Jiang Y, Sun X, Tao Y, Hu Y, Li C, Wang Q, Wang Y, Chen CD, Shi Y, and Zhang X. 2015. The histone H3 lysine-27 demethylase Jmjd3 plays a critical role in specific regulation of Th17 cell differentiation. J Mol Cell Biol 7: 505–516. [PubMed: 25840993]
53. Li Q, Zou J, Wang M, Ding X, Chepelev I, Zhou X, Zhao W, Wei G, Cui J, Zhao K, Wang HY, and Wang RF. 2014. Critical role of histone demethylase Jmjd3 in the regulation of CD4+ T-cell differentiation. Nat Commun 5: 5780. [PubMed: 25531312]

54. Yamada T, Nabe S, Toriyama K, Suzuki J, Inoue K, Imai Y, Shiraishi A, Takenaka K, Yasukawa M, and Yamashita M. 2019. Histone H3K27 Demethylase Negatively Controls the Memory Formation of Antigen-Stimulated CD8(+) T Cells. J Immunol 202: 1088–1098. [PubMed: 30626691]
55. Beyaz S, Kim JH, Pinello L, Xifaras ME, Hu Y, Huang J, Kerenyi MA, Das PP, Barnitz RA, Herault A, Dogum R, Haining WN, Yilmaz OH, Passegue E, Yuan GC, Orkin SH, and Winau F. 2017. The histone demethylase UTX regulates the lineage-specific epigenetic program of invariant natural killer T cells. Nat Immunol 18: 184–195. [PubMed: 27992400]
56. Northrup D, Yagi R, Cui K, Proctor WR, Wang C, Placek K, Pohl LR, Wang R, Ge K, Zhu J, and Zhao K. 2017. Histone demethylases UTX and JMJD3 are required for NKT cell development in mice. Cell Biosci 7: 25. [PubMed: 28529687]
57. Bjornsson HT 2015. The Mendelian disorders of the epigenetic machinery. Genome Res 25: 1473–1481. [PubMed: 26430157]
58. Stagi S, Gulino AV, Lapi E, and Rigante D. 2016. Epigenetic control of the immune system: a lesson from Kabuki syndrome. Immunol Res 64: 345–359. [PubMed: 26411453]
59. Li X, Zhang Y, Zheng L, Liu M, Chen CD, and Jiang H. 2018. UTX is an escape from X-inactivation tumor-suppressor in B cell lymphoma. Nat Commun 9: 2720. [PubMed: 30006524]
60. Pawlyn C, Kaiser MF, Heuck C, Melchor L, Wardell CP, Murison A, Chavan SS, Johnson DC, Begum DB, Dahir NM, Proszek PZ, Cairns DA, Boyle EM, Jones JR, Cook G, Drayson MT, Owen RG, Gregory WM, Jackson GH, Barlogie B, Davies FE, Walker BA, and Morgan GJ. 2016. The Spectrum and Clinical Impact of Epigenetic Modifier Mutations in Myeloma. Clin Cancer Res 22: 5783–5794. [PubMed: 27235425]
61. van Haaften G, Dalgliesh GL, Davies H, Chen L, Bignell G, Greenman C, Edkins S, Hardy C, O'Meara S, Teague J, Butler A, Hinton J, Latimer C, Andrews J, Barthorpe S, Beare D, Buck G, Campbell PJ, Cole J, Forbes S, Jia M, Jones D, Kok CY, Leroy C, Lin ML, McBride DJ, Maddison M, Maquire S, McLay K, Menzies A, Mironenko T, Mulderrig L, Mudie L, Pleasance E, Shepherd R, Smith R, Stebbings L, Stephens P, Tang G, Tarpey PS, Turner R, Turrell K, Varian J, West S, Widaa S, Wray P, Collins VP, Ichimura K, Law S, Wong J, Yuen ST, Leung SY, Tonon G, DePinho RA, Tai YT, Anderson KC, Kahnoski RJ, Massie A, Khoo SK, Teh BT, Stratton MR, and Futreal PA. 2009. Somatic mutations of the histone H3K27 demethylase gene UTX in human cancer. Nat Genet 41: 521–523. [PubMed: 19330029]
62. Ezponda T, Dupere-Richer D, Will CM, Small EC, Varghese N, Patel T, Nabet B, Popovic R, Oyer J, Bulic M, Zheng Y, Huang X, Shah MY, Maji S, Riva A, Occhionorelli M, Tonon G, Kelleher N, Keats J, and Licht JD. 2017. UTX/KDM6A Loss Enhances the Malignant Phenotype of Multiple Myeloma and Sensitizes Cells to EZH2 inhibition. Cell Rep 21: 628–640. [PubMed: 29045832]
63. Anderton JA, Bose S, Vockerodt M, Vrzalikova K, Wei W, Kuo M, Helin K, Christensen J, Rowe M, Murray PG, and Woodman CB. 2011. The H3K27me3 demethylase, KDM6B, is induced by Epstein-Barr virus and over-expressed in Hodgkin's Lymphoma. Oncogene 30: 2037–2043. [PubMed: 21242977]
64. Zhang Y, Shen L, Stupack DG, Bai N, Xun J, Ren G, Han J, Li L, Luo Y, Xiang R, and Tan X. 2016. JMJD3 promotes survival of diffuse large B-cell lymphoma subtypes via distinct mechanisms. Oncotarget 7: 29387–29399. [PubMed: 27102442]
65. Mathur R, Sehgal L, Havranek O, Kohrer S, Khashab T, Jain N, Burger JA, Neelapu SS, Davis RE, and Samaniego F. 2017. Inhibition of demethylase KDM6B sensitizes diffuse large B-cell lymphoma to chemotherapeutic drugs. Haematologica 102: 373–380. [PubMed: 27742770]
66. Yoon HS, Scharer CD, Majumder P, Davis CW, Butler R, Zinzow-Kramer W, Skountzou I, Koutsonanos DG, Ahmed R, and Boss JM. 2012. ZBTB32 is an early repressor of the CIITA and MHC class II gene expression during B cell differentiation to plasma cells. J Immunol 189: 2393–2403. [PubMed: 22851713]
67. Subramanian A, Tamayo P, Mootha VK, Mukherjee S, Ebert BL, Gillette MA, Paulovich A, Pomeroy SL, Golub TR, Lander ES, and Mesirov JP. 2005. Gene set enrichment analysis: a knowledge-based approach for interpreting genome-wide expression profiles. Proc Natl Acad Sci U S A 102: 15545–15550. [PubMed: 16199517]
68. Haines RR, Barwick BG, Scharer CD, Majumder P, Randall TD, and Boss JM. 2018. The Histone Demethylase LSD1 Regulates B Cell Proliferation and Plasmablast Differentiation. J Immunol 201: 2799–2811. [PubMed: 30232138]

69. Kruidenier L, Chung CW, Cheng Z, Liddle J, Che K, Joberty G, Bantscheff M, Bountra C, Bridges A, Diallo H, Eberhard D, Hutchinson S, Jones E, Katso R, Leveridge M, Mander PK, Mosley J, Ramirez-Molina C, Rowland P, Schofield CJ, Sheppard RJ, Smith JE, Swales C, Tanner R, Thomas P, Tumber A, Drewes G, Oppermann U, Patel DJ, Lee K, and Wilson DM. 2012. A selective jumonji H3K27 demethylase inhibitor modulates the proinflammatory macrophage response. Nature 488: 404–408. [PubMed: 22842901]
70. Gloury R, Zotos D, Zuidscherwoude M, Masson F, Liao Y, Hasbold J, Corcoran LM, Hodgkin PD, Belz GT, Shi W, Nutt SL, Tarlinton DM, and Kallies A. 2016. Dynamic changes in Id3 and E-protein activity orchestrate germinal center and plasma cell development. J Exp Med 213: 1095–1111. [PubMed: 27217539]
71. Heinemann B, Nielsen JM, Hudlebusch HR, Lees MJ, Larsen DV, Boesen T, Labelle M, Gerlach LO, Birk P, and Helin K. 2014. Inhibition of demethylases by GSK-J1/J4. Nature 514: E1–2. [PubMed: 25279926]
72. Serrano M, Hannon GJ, and Beach D. 1993. A new regulatory motif in cell-cycle control causing specific inhibition of cyclin D/CDK4. Nature 366: 704–707. [PubMed: 8259215]
73. Kubbutat MH, Jones SN, and Vousden KH. 1997. Regulation of p53 stability by Mdm2. Nature 387: 299–303. [PubMed: 9153396]
74. Chinnadurai G, Vijayalingam S, and Gibson SB. 2008. BNIP3 subfamily BH3-only proteins: mitochondrial stress sensors in normal and pathological functions. Oncogene 27 Suppl 1: S114–127. [PubMed: 19641497]
75. Saunier E, Benelli C, and Bortoli S. 2016. The pyruvate dehydrogenase complex in cancer: An old metabolic gatekeeper regulated by new pathways and pharmacological agents. Int J Cancer 138: 809–817. [PubMed: 25868605]
76. Holness MJ, and Sugden MC. 2003. Regulation of pyruvate dehydrogenase complex activity by reversible phosphorylation. Biochem Soc Trans 31: 1143–1151. [PubMed: 14641014]
77. Shi W, Liao Y, Willis SN, Taubenheim N, Inouye M, Tarlinton DM, Smyth GK, Hodgkin PD, Nutt SL, and Corcoran LM. 2015. Transcriptional profiling of mouse B cell terminal differentiation defines a signature for antibody-secreting plasma cells. Nat Immunol 16: 663–673. [PubMed: 25894659]
78. Ito K, and Groudine M. 1997. A new member of the cationic amino acid transporter family is preferentially expressed in adult mouse brain. J Biol Chem 272: 26780–26786. [PubMed: 9334265]
79. Vekony N, Wolf S, Boissel JP, Gnauert K, and Closs EI. 2001. Human cationic amino acid transporter hCAT-3 is preferentially expressed in peripheral tissues. Biochemistry 40: 12387–12394. [PubMed: 11591158]
80. Lu Y, O'Dowd BF, Orrego H, and Israel Y. 1992. Cloning and nucleotide sequence of human liver cDNA encoding for cystathionine gamma-lyase. Biochem Biophys Res Commun 189: 749–758. [PubMed: 1339280]
81. Sohm B, Sissler M, Park H, King MP, and Florentz C. 2004. Recognition of human mitochondrial tRNALeu(UUR) by its cognate leucyl-tRNA synthetase. J Mol Biol 339: 17–29. [PubMed: 15123417]
82. Merk M, Mitchell RA, Endres S, and Bucala R. 2012. D-dopachrome tautomerase (D-DT or MIF-2): doubling the MIF cytokine family. Cytokine 59: 10–17. [PubMed: 22507380]
83. Wang X, Yang R, Jadhao SB, Yu D, Hu H, Glynn-Cunningham N, Sztalryd C, Silver KD, and Gong DW. 2012. Transmembrane emp24 protein transport domain 6 is selectively expressed in pancreatic islets and implicated in insulin secretion and diabetes. Pancreas 41: 10–14. [PubMed: 22129529]
84. Stambolian D, Ai Y, Sidjanin D, Nesburn K, Sathe G, Rosenberg M, and Bergsma DJ. 1995. Cloning of the galactokinase cDNA and identification of mutations in two families with cataracts. Nat Genet 10: 307–312. [PubMed: 7670469]
85. Webb G, Vaska V, Coggan M, and Board P. 1996. Chromosomal localization of the gene for the human theta class glutathione transferase (GSTT1). Genomics 33: 121–123. [PubMed: 8617495]

86. Allikmets R, Gerrard B, Hutchinson A, and Dean M. 1996. Characterization of the human ABC superfamily: isolation and mapping of 21 new genes using the expressed sequence tags database. Hum Mol Genet 5: 1649–1655. [PubMed: 8894702]

87. Kee BL 2009. E and ID proteins branch out. Nat Rev Immunol 9: 175–184. [PubMed: 19240756]

88. Willis SN, Tellier J, Liao Y, Trezise S, Light A, O'Donnell K, Garrett-Sinha LA, Shi W, Tarlinton DM, and Nutt SL. 2017. Environmental sensing by mature B cells is controlled by the transcription factors PU.1 and SpiB. Nat Commun 8: 1426. [PubMed: 29127283]

89. Zhang Y, and Good-Jacobson KL. 2019. Epigenetic regulation of B cell fate and function during an immune response. Immunol Rev 288: 75–84. [PubMed: 30874352]

90. Zhang J, Dominguez-Sola D, Hussein S, Lee JE, Holmes AB, Bansal M, Vlasevska S, Mo T, Tang H, Basso K, Ge K, Dalla-Favera R, and Pasqualucci L. 2015. Disruption of KMT2D perturbs germinal center B cell development and promotes lymphomagenesis. Nat Med 21: 1190–1198. [PubMed: 26366712]

91. Hatzi K, Geng H, Doane AS, Meydan C, LaRiviere R, Cardenas M, Duy C, Shen H, Vidal MNC, Baslan T, Mohammad HP, Kruger RG, Shaknovich R, Haberman AM, Inghirami G, Lowe SW, and Melnick AM. 2019. Histone demethylase LSD1 is required for germinal center formation and BCL6-driven lymphomagenesis. Nat Immunol 20: 86–96. [PubMed: 30538335]

92. Cheng Y, He C, Wang M, Ma X, Mo F, Yang S, Han J, and Wei X. 2019. Targeting epigenetic regulators for cancer therapy: mechanisms and advances in clinical trials. Signal Transduct Target Ther 4: 62. [PubMed: 31871779]

93. Tran N, Broun A, and Ge K. 2020. Lysine demethylase KDM6A in differentiation, development and cancer. Mol Cell Biol.

94. Duan R, Du W, and Guo W. 2020. EZH2: a novel target for cancer treatment. J Hematol Oncol 13: 104. [PubMed: 32723346]

95. Li Y, Zhang M, Sheng M, Zhang P, Chen Z, Xing W, Bai J, Cheng T, Yang FC, and Zhou Y. 2018. Therapeutic potential of GSK-J4, a histone demethylase KDM6B/JMJD3 inhibitor, for acute myeloid leukemia. J Cancer Res Clin Oncol 144: 1065–1077. [PubMed: 29594337]

96. Taube JH, Sphyris N, Johnson KS, Reisenauer KN, Nesbit TA, Joseph R, Vijay GV, Sarkar TR, Bhangre NA, Song JJ, Chang JT, Lee MG, Soundararajan R, and Mani SA. 2017. The H3K27me3-demethylase KDM6A is suppressed in breast cancer stem-like cells, and enables the resolution of bivalency during the mesenchymal-epithelial transition. Oncotarget 8: 65548–65565. [PubMed: 29029452]

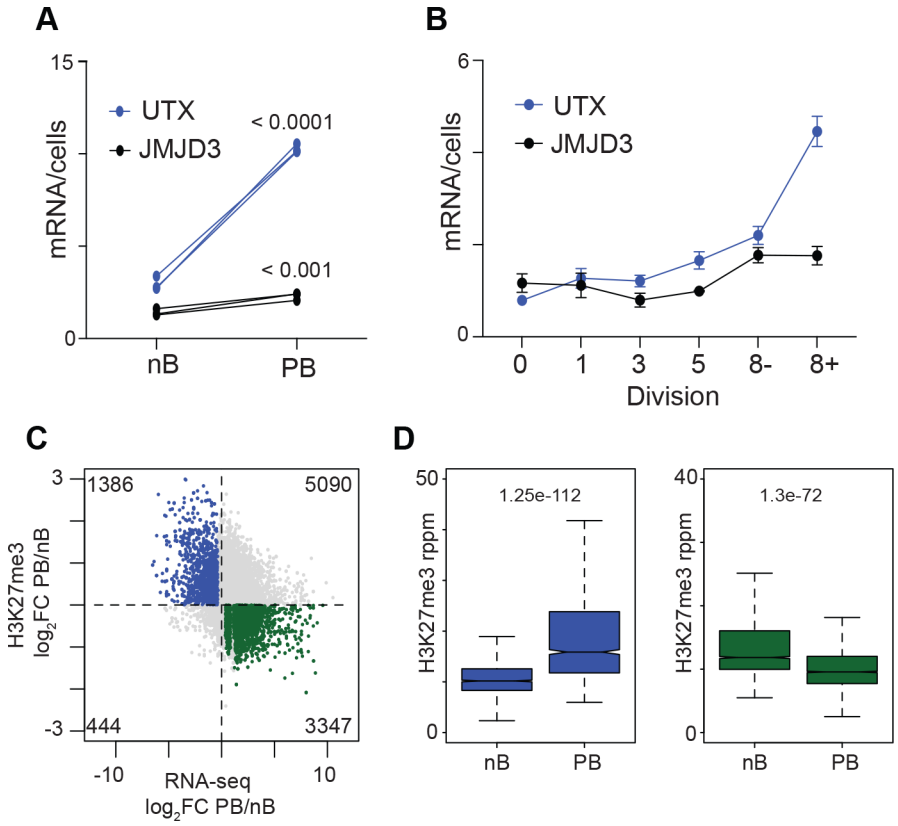

Figure 1 –. H3K27me3 demethylases are upregulated during B cell differentiation.

(**A**) Expression in mRNA/cell of *Utx* and *Jmjd3* in control nB and PB (Haines *et al.* 2018). (**B**) Expression in mRNA/cell of *Utx* and *Jmjd3* per division (Barwick *et al.* 2016). (**C**) The log_2FC change in gene expression between PB and nB (Haines *et al.* 2018) was plotted against the log_2FC change in H3K27me3 between PB and nB (Guo et al. 2018). The total number of unique genes in each quadrant is indicated. (**D**) Quantification of H3K27me3 levels in PB and nB

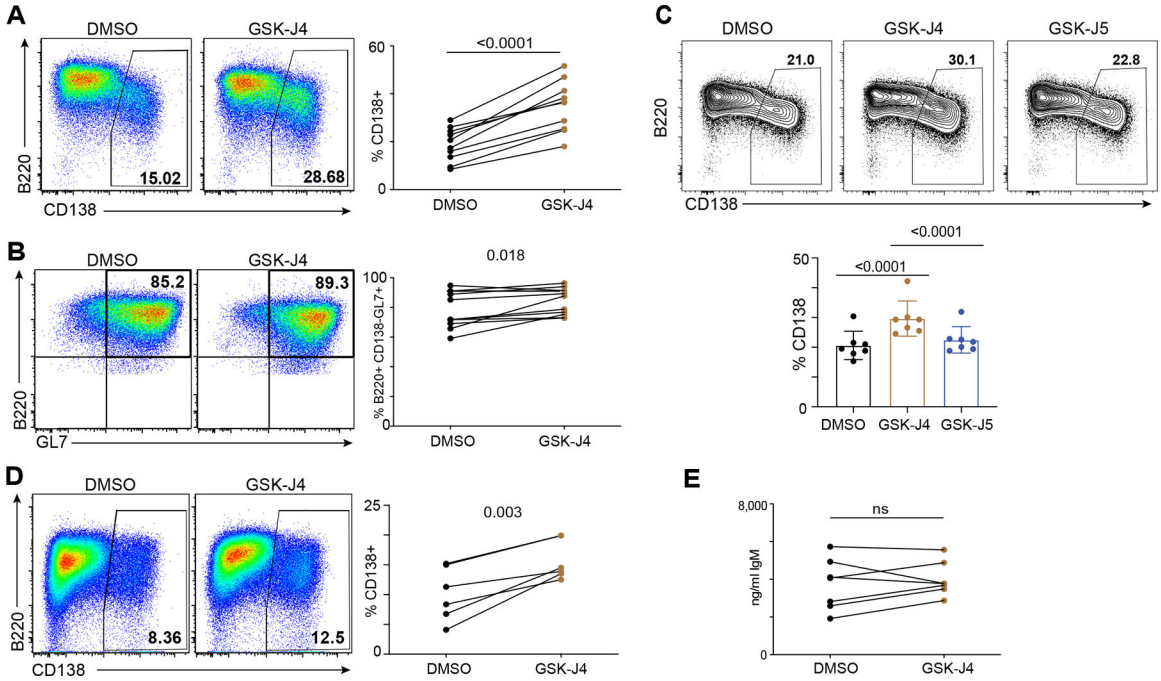

Figure 2 –. GSK-J4 treatment leads to an increase in the frequency of CD138+ plasmablasts.

Representative plots and quantitation of the frequency of (**A**) CD138+ PB and (**B**) CD138−B220+GL7+ ActB after 3 days of *ex vivo* stimulation with LPS, IL-2, IL-5 in the presence of 250 nM GSK-J4 or DMSO control. (**C**) Representative plots and quantitation of the frequency of CD138+ PB after 3 days of *ex vivo* stimulation with LPS, IL-2, IL-5 in the presence of 250 nM GSK-J4, 250 nM GSK-J5 (inactive compound), or DMSO. (**D**) Frequency of CD138+ PB at day four of *ex vivo* culture with CD40L, IL-4, IL-5 in the presence of 250 nM GSK-J4 or DMSO. (**E**) IgM antibody titers after 2.5 hr incubation of magnetically enriched PB from DMSO or 250 nM GSK-J4 treated cultures. Data are from two independent experiments with 3–4 mice each. Significance was determined by paired two-tailed Student's *t* test.

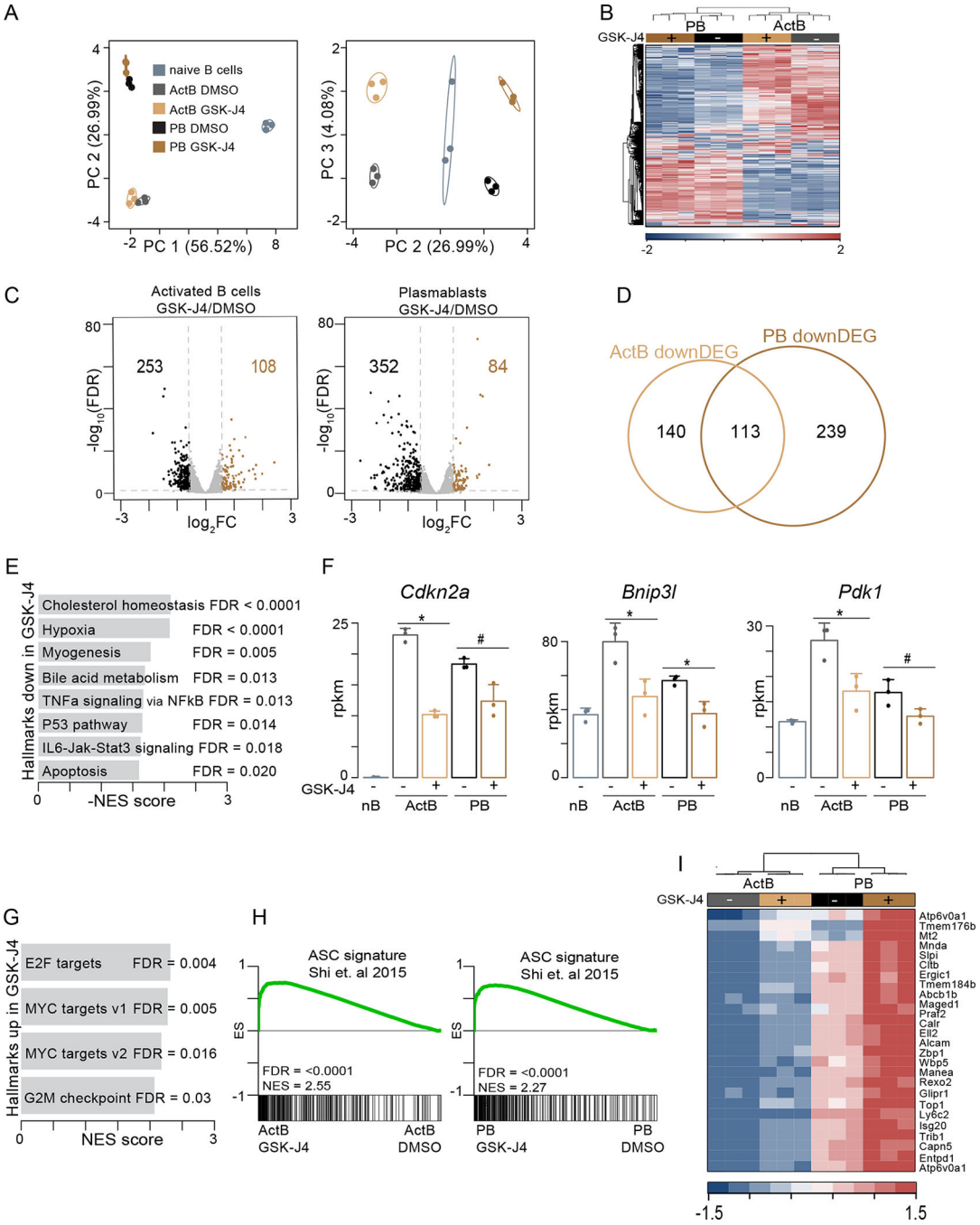

Figure 3 –. Inhibition of UTX and JMJD3 leads to global changes in gene expression.

RNA sequencing was performed on magnetically enriched ActB and PB from DMSO or 250 nM GSK-J4 treated cultures as well as naïve B cell controls. (**A**) Principal component analysis of 10, 031 genes differentially expressed in a least one comparison RNA-seq data. The percentage in parentheses is the proportion of variation explained by each component and circles represent 99% confidence intervals for each group. (**B**) Hierarchical clustering of samples and DEG (FDR < 0.05, 1.5-fold change) between inhibitor GSK-J4 and DMSO cells. (**C**) Volcano plots of DEG (FDR < 0.05, 1.5-fold change) between GSK-J4 and

DMSO treated ActB (left) and PB (right). (**D**) Venn diagram representing the overlap of ActB and PB downDEG between inhibitor and DMSO treated cells. (**E**) Hallmark gene sets downregulated upon treatment with GSK-J4 treated ActB. GSEA was performed on a ranked gene list comparing ActB GSK-J4 vs DMSO treated cells. (**F**) Examples of genes downregulated in GSK-J4 treated cells. (**G**) Hallmark gene sets upregulated in GSK-J4 treated ActB. (**H**) GSEA for a previously defined ASC-signature genes (Shi *et al.* 2015) in GSK-J4 treated ActB (left) and PB (right) versus control. (**I**) Heatmap showing the expression of the top 25 DEG from the ASC-signature gene set from (H) in GSK-J4 and DMSO treated ActB and PB. Data represent the mean of three biological replicates per group. * FDR < 0.05 and >1.5 fold change, # FDR < 0.05 with <1.5 fold change

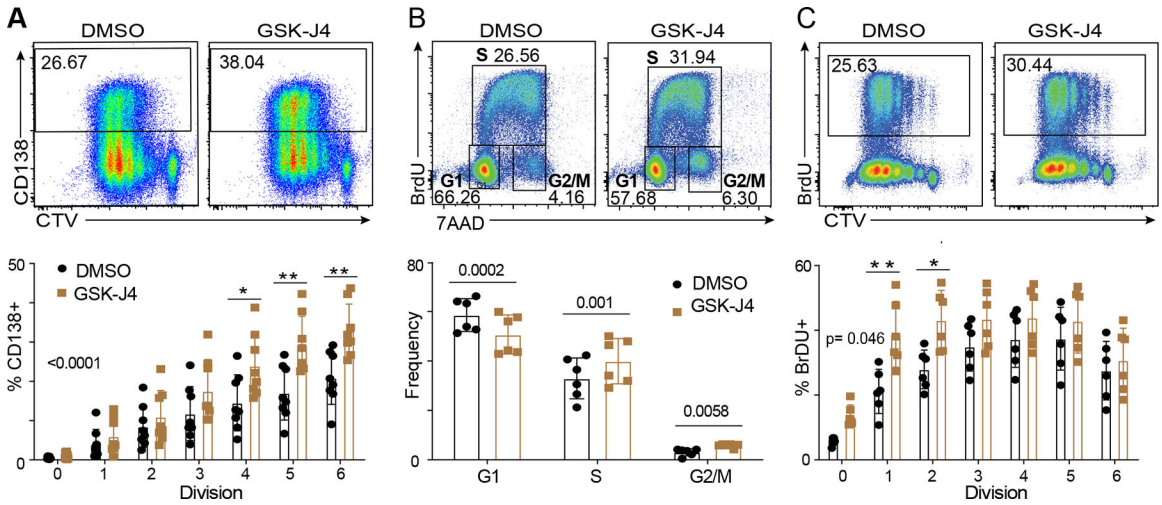

Figure 4 –. Inhibition of UTX and JMJD3 promotes cell proliferation

(**A**) Representative plots of CD138 versus CTV after three days of *ex vivo* culture (top) and quantification of the frequency of CD138+ plasmablasts per cell division (bottom) at day 3 of *ex vivo* stimulation. (**B**) Frequency of cells at G1 (2N, BrdU-), S (BrdU+), and G2/M (4N, BrdU-) phases of the cell cycle following two-hour incubation with BrDU at day 3 of *ex vivo* stimulation in the presence of GSK-J4 or DMSO. (**C**) Representative plots of BrdU versus CTV for GSK-J4 and DMSO treated cells (top) with quantification of BrdU+ cells per division (bottom). Data are summary of two independent experiments with 3–4 mice each. Significance was determined by paired two-tailed Student's *t* test (B) and two-way ANOVA followed by Sidak's multiple comparisons test A,C). * p-value < 0.05, ** p-value <0.001.

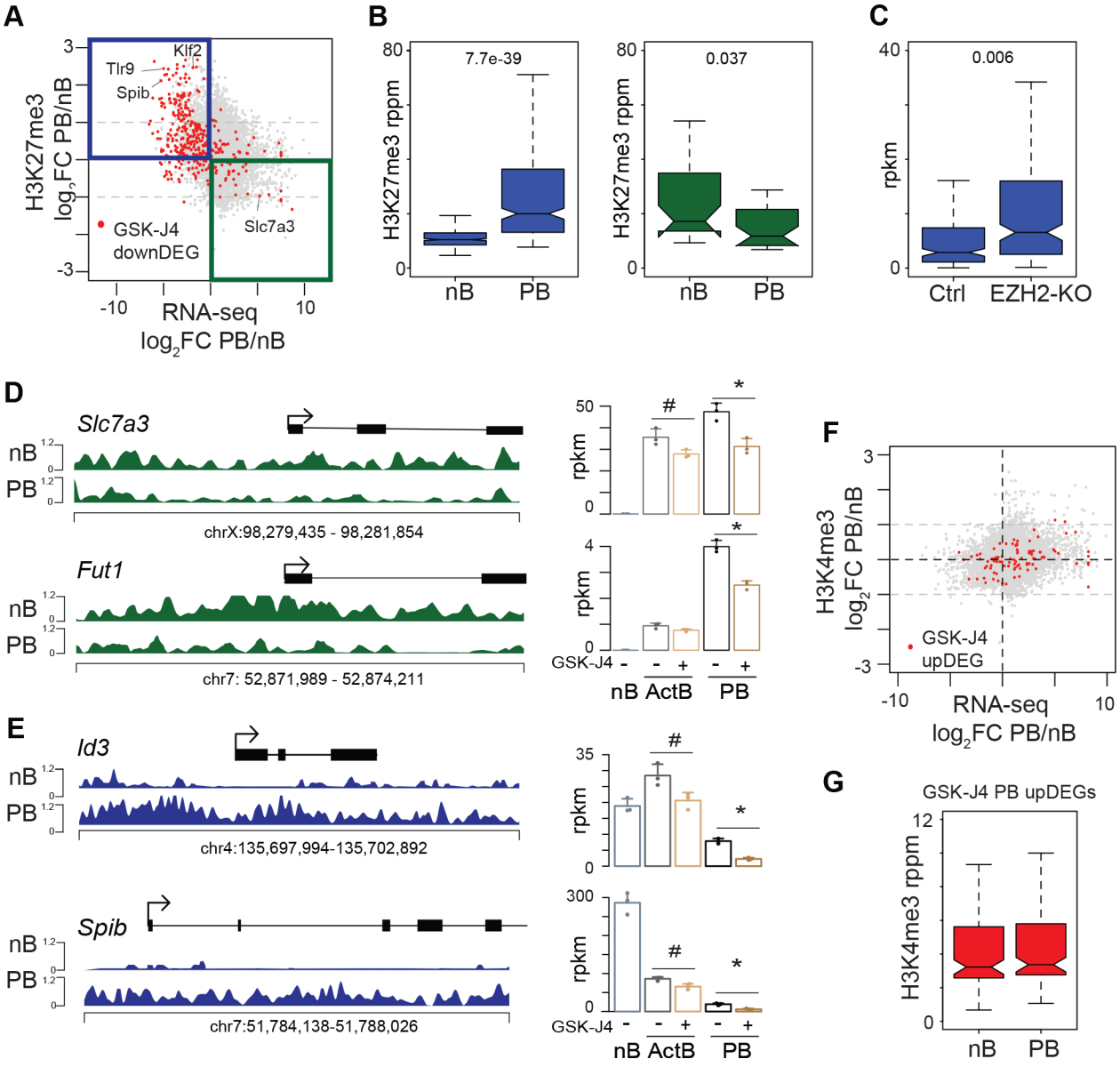

Figure 5 –. DEGs are enriched for genes regulated by H3K27me3 levels.

(**A**) The $\log_2$FC change in gene expression PB and nB (Haines *et al.* 2018) was plotting against the $\log_2$FC change in H3K27me3 between PB and nB (Guo et al. 2018) as in Figure 1. GSK-J4 downDEG in PB comparison were represented by red dots. (**B**) Quantification of H3K27me3 levels in wild type nB and PB at GSK-J4 downDEG. (**C**) Average expression of GSK-J4 downDEG in the "blue" quadrant in A in EZH2-sufficient and -deficient PB (Guo et al. 2018). (**D, E**) Examples of GSK-J4 downDEG regulated by H3K27me3 levels. * FDR < 0.05 and >1.5 fold change, # FDR < 0.05 with <1.5 fold change. (**F**) The $\log_2$FC change in gene expression PB and nB (Haines *et al.* 2018) was plotting against the $\log_2$FC change in H3K4me3 between PB and nB (Scharer et al. 2018). GSK-J4 upDEG in PB comparison were represented by red dots. (**G**) Quantification of H3K4me3 levels in wild type nB and PB at GSK-J4 upDEG.